

# Potential of Data Driven Methods for Reynolds Stress Modeling - A Fundamental View

Bernhard Eisfeld<sup>†</sup>, DLR

Symposium on Turbulence Modeling:  
Roadblocks and the Potential for Machine Learning  
27-29 July 2022

<sup>†</sup> Sadly, Bernhard passed away on the 26th of January 2022, a few days after the completion of this work.

# Overview

- Introduction
- Theory
- Reynolds Stress Modeling
- Simulation Results
  - Fundamental Flows
  - Applications
- Potential of Data Driven Methods
- Conclusion



# Overview

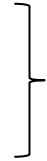
- **Introduction**
- Theory
- Reynolds Stress Modeling
- Simulation Results
  - Fundamental Flows
  - Applications
- Potential of Data Driven Methods
- Conclusion



# Introduction

## RANS Models

- No limitations on
  - Reynolds number
  - Geometric complexity
- Limitations on
  - Accuracy (separation)



Indispensable in

- Industrial application
- Aerodynamic design

Requirements

- Improved accuracy
- Design: single model for various flow conditions

From theory:  
Fundamental conditions → Calibration  
Turbulent equilibrium

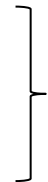


potential  
conflict

## Data Driven Turbulence Modeling

Idea

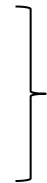
- Real data
- Artificial intelligence (machine learning)



- No limitation to canonical flows for learning
- Improved predictions in application

Method

- Optimisation of
  - Model coefficients
  - Functional dependence of coefficients
  - Model form (additional terms)



Unlimited improvement?



# Overview

- Introduction
- **Theory**
- Reynolds Stress Modeling
- Simulation Results
  - Fundamental Flows
  - Applications
- Potential of Data Driven Methods
- Conclusion



# Theory

## Turbulent Equilibrium

- High Reynolds number
  - Boundary layer assumptions
- Simplification of turbulence equations
- $$\begin{cases} 0 = P_{ij} + \Pi_{ij} - \varepsilon_{ij} & \text{Reynolds stress equation} \\ 0 = P^{(k)} - \varepsilon & \text{k-equation.} \end{cases}$$

Turbulent equilibrium

## Reynolds Stress Modeling

- Pressure strain correlation (off walls)

$$\Pi_{ij} = \underbrace{\varepsilon A_{ij}}_{\text{slow}} + k \underbrace{M_{ijkl} \frac{\partial U_k}{\partial x_l}}_{\text{rapid}}$$

with  $A_{ij}, M_{ijkl} = f(b_{pq})$

functions of  
Reynolds stress anisotropies

- Dissipation (high Re)

$$\varepsilon_{ij} = \frac{2}{3} \varepsilon \delta_{ij}$$

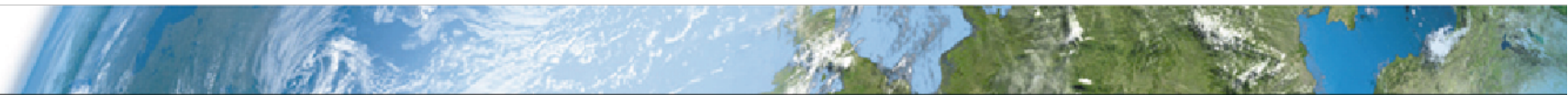
isotropic

## 2D Mean Flow

- Only one velocity gradient

$$\frac{\partial U_k}{\partial x_l} \rightarrow \frac{\partial U}{\partial y}$$

- ↓
- 3 **algebraic** equations for  $b_{11}|_{eq}, b_{22}|_{eq}, b_{12}|_{eq} = f(C_i)$   
with  $C_i$  = coeff. of pressure-strain model
  - **Independent of velocity profile**  
→ valid for any 2D flow in turbulent equilibrium



# Overview

- Introduction
- Theory
- **Reynolds Stress Modeling**
- Simulation Results
  - Fundamental Flows
  - Applications
- Potential of Data Driven Methods
- Conclusion





# Reynolds Stress Model

## Pressure Strain Correlation Models

- SSG
 
$$\Pi_{ij} = -\varepsilon \left( C_1 + C_1^* \frac{P^{(k)}}{\varepsilon} \right) b_{ij} + C_2 \varepsilon \left( b_{ik} b_{kj} - \frac{1}{3} b_{kl} b_{kl} \delta_{ij} \right) + (C_3 - C_3^* \sqrt{II_b}) k S_{ij} \\ + C_4 k \left( b_{ik} S_{jk} + b_{jk} S_{ik} - \frac{2}{3} b_{kl} S_{kl} \delta_{ij} \right) + C_5 k (b_{ik} \Omega_{jk} + b_{jk} \Omega_{ik})$$
 Full model.
- Simplification 1
 
$$\Pi_{ij} = -\varepsilon \left( C_1 + C_1^* \cancel{\frac{P^{(k)}}{\varepsilon}} \right) b_{ij} + C_2 \varepsilon \left( b_{ik} b_{kj} - \frac{1}{3} b_{kl} b_{kl} \delta_{ij} \right) + (C_3 - C_3^* \sqrt{II_b}) k S_{ij} \\ + C_4 k \left( b_{ik} S_{jk} + b_{jk} S_{ik} - \frac{2}{3} b_{kl} S_{kl} \delta_{ij} \right) + C_5 k (b_{ik} \Omega_{jk} + b_{jk} \Omega_{ik})$$
 Reduce non-linearity
- Simplification 2
 
$$\Pi_{ij} = -\varepsilon \left( C_1 + C_1^* \frac{P^{(k)}}{\varepsilon} \right) b_{ij} + C_2 \varepsilon \left( b_{ik} b_{kj} - \frac{1}{3} b_{kl} b_{kl} \delta_{ij} \right) + (C_3 - C_3^* \cancel{\sqrt{II_b}}) k S_{ij} \\ + C_4 k \left( b_{ik} S_{jk} + b_{jk} S_{ik} - \frac{2}{3} b_{kl} S_{kl} \delta_{ij} \right) + C_5 k (b_{ik} \Omega_{jk} + b_{jk} \Omega_{ik})$$
 Remove dependence on invariants
- Simplification 3
 
$$\Pi_{ij} = -\varepsilon C_1 b_{ij} + C_2 \varepsilon \left( b_{ik} b_{kj} - \frac{1}{3} b_{kl} b_{kl} \delta_{ij} \right) + C_3 k S_{ij}$$
 Drastic surgery





# Reynolds Stress Model

## Calibration

- Strategy
  - Consider equilibrium state of original SSG model → invariants/eigenvalues of anisotropy tensor
  - Rotate principal axes of anisotropy tensor to target  $b_{12}|_{eq}$  → maintain invariants/eigenvalues
- Equilibrium states

	$b_{11} _{eq}$	$b_{22} _{eq}$	$b_{12} _{eq}$
Set 1	0.2099	-0.1355	-0.1506
Set 2	0.2007	-0.1266	-0.1603
Set 3	0.1907	-0.1165	-0.1700

Reduced momentum transfer

Original SSG model

Increased momentum transfer

→ 12 different models (4 model forms x 3 sets of coefficients)

→ Equilibrium values of  $II_b, III_b$  virtually identical

## Length-scale equation

- BSL- $\omega$ -equation (Menter, 1994)
- Length-scale correction (Eisfeld & Rumsey, 2020)



# Overview

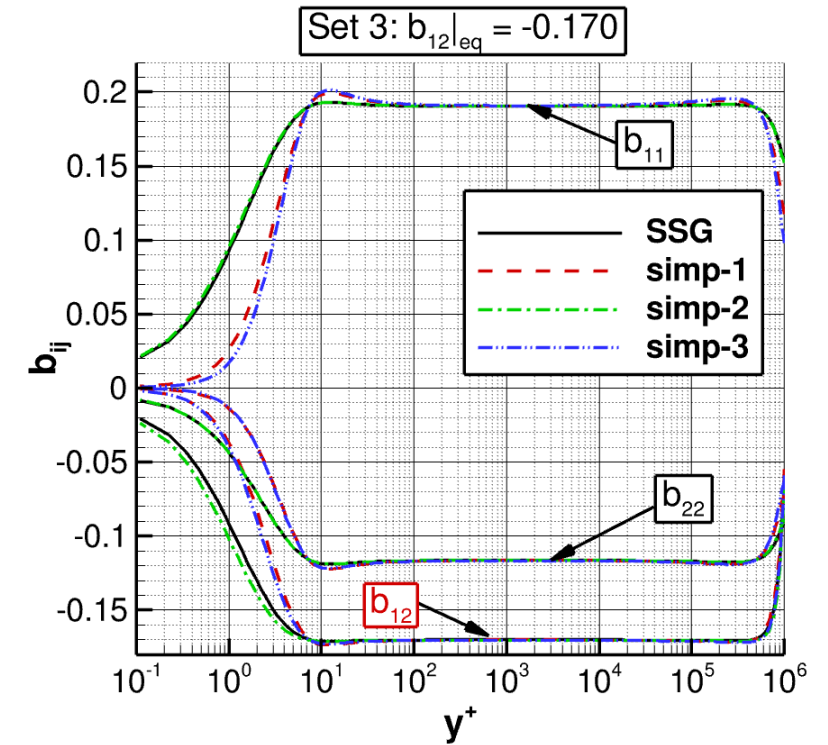
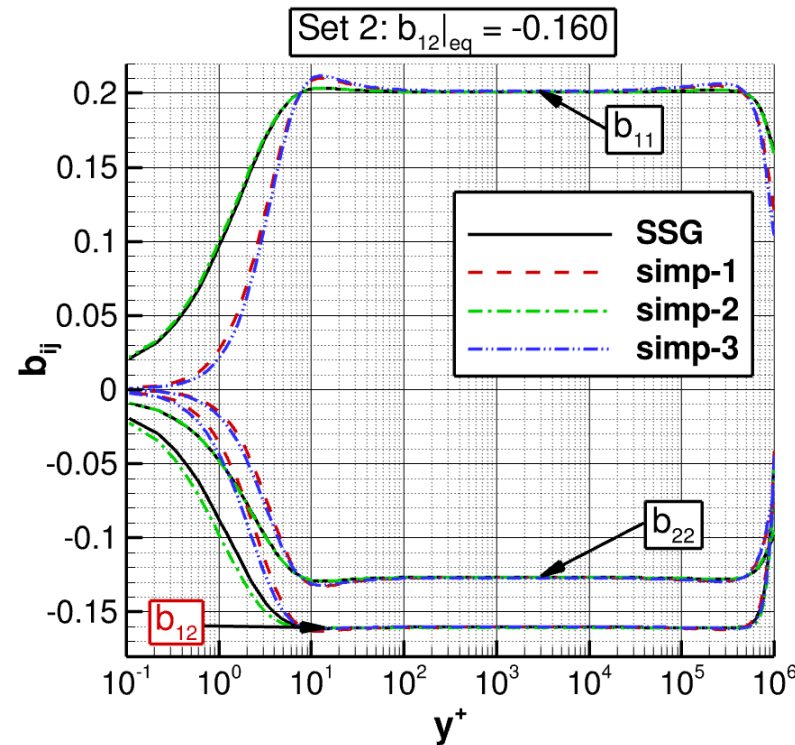
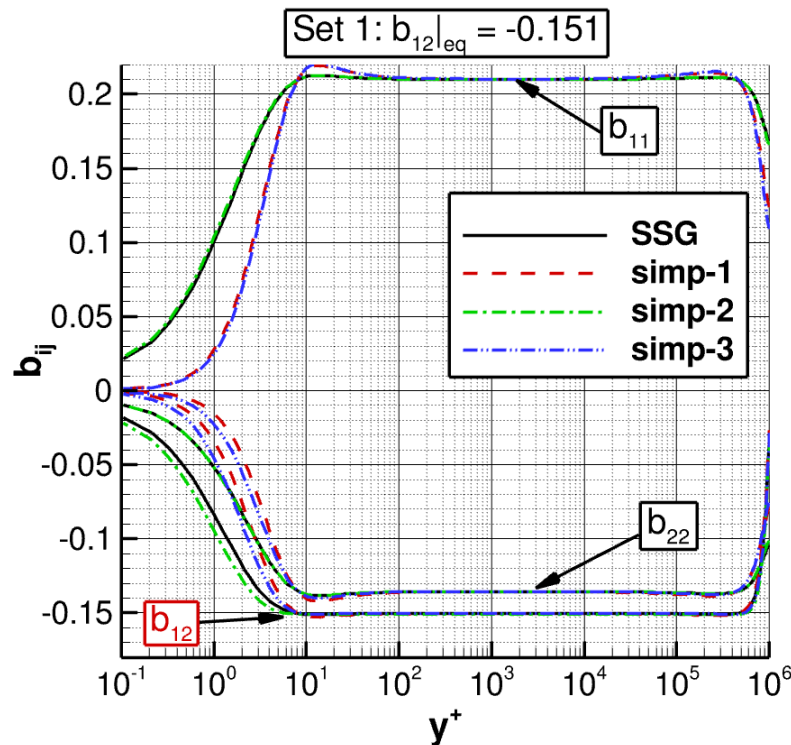
- Introduction
- Theory
- Reynolds Stress Modeling
- **Simulation Results**
  - **Fundamental Flows**
  - Applications
- Potential of Data Driven Methods
- Conclusion



# Simulation Results: Fundamental Flows

## Channel Flow at $Re_H = 80e6$ (1)

- Reynolds stress anisotropies



- Wide range of constant  $b_{ij}|_{eq} = \text{target } b_{ij}|_{eq}$
- Equilibrium state independent of model form

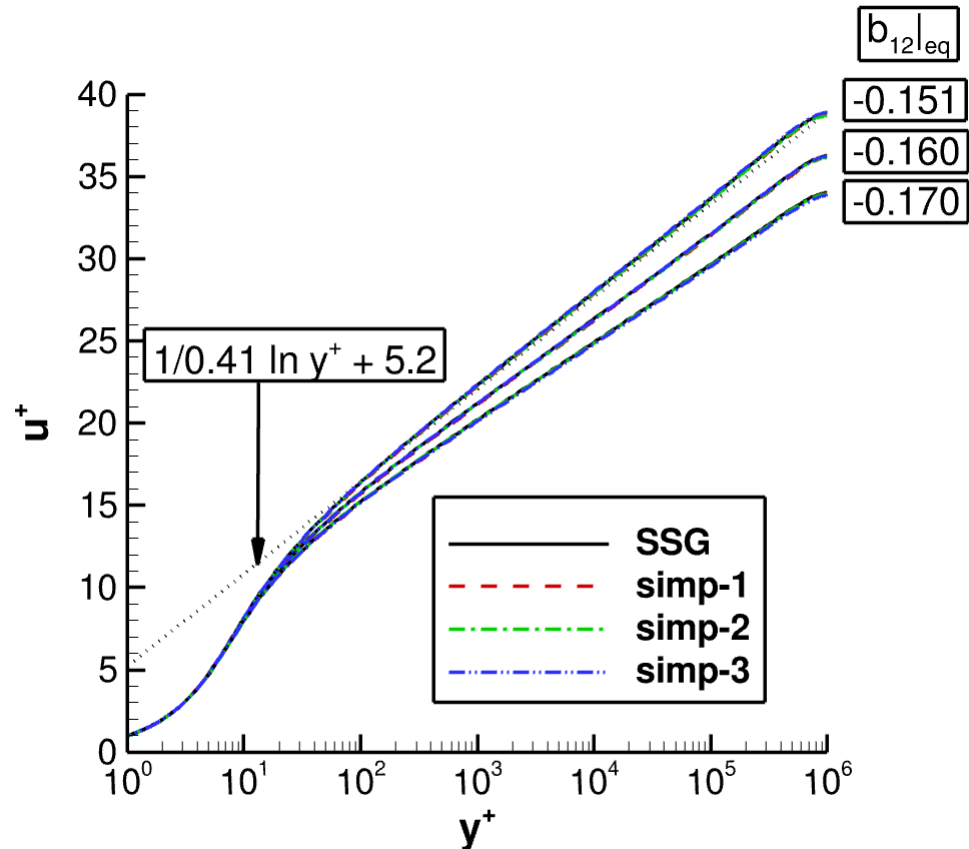
→ Equilibrium state confirmed  
→ Theory confirmed

→ Calibration strategy successful

# Simulation Results: Fundamental Flows

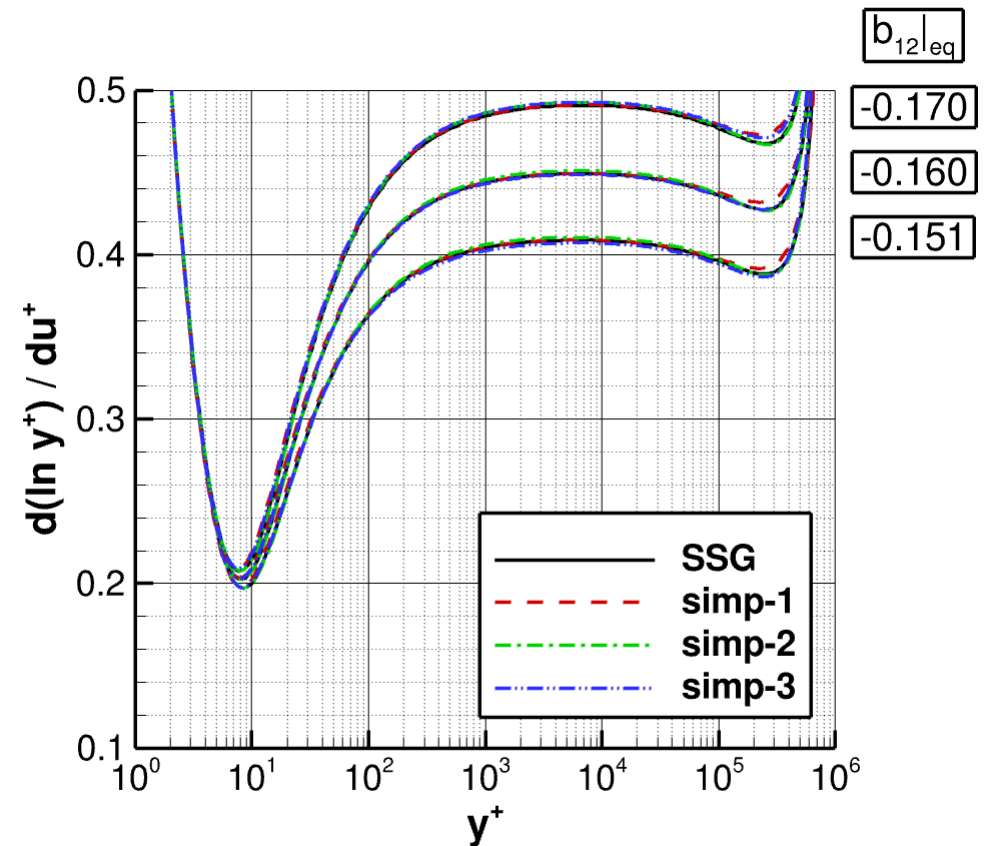
## Channel Flow at $Re_H = 80e6$ (2)

- Log-law



- Determined by equilibrium state
- independent of model form

- Von-Karman constant

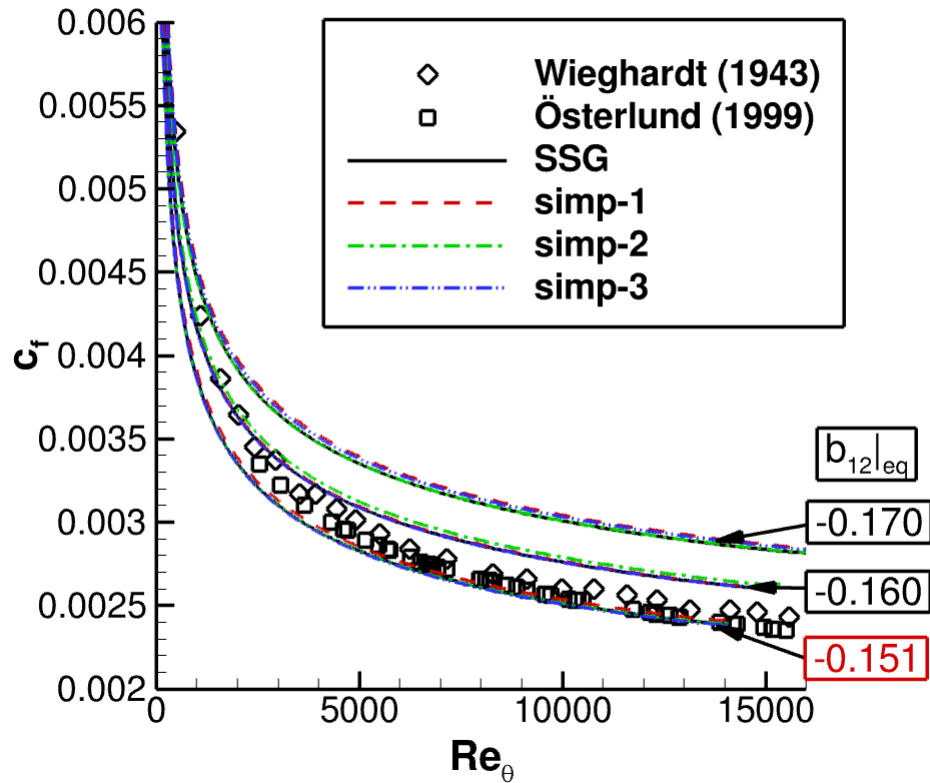


- $\kappa = f(b_{12}|_{eq})$   
cf. Abid & Speziale (1993)

# Simulation Results: Fundamental Flows

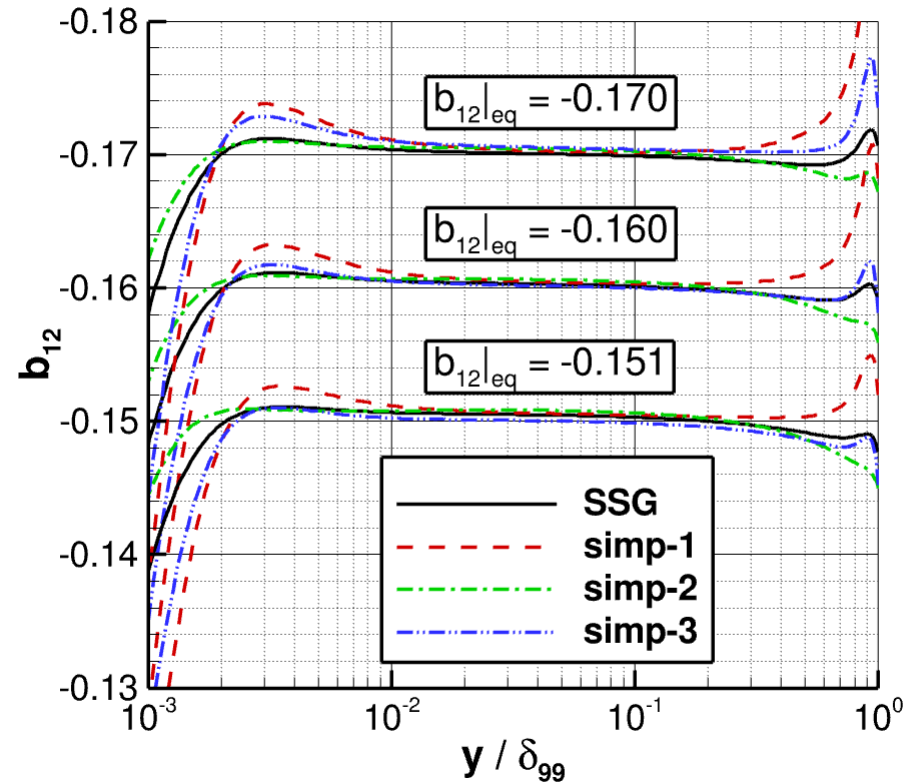
## Zero Pressure Gradient Boundary Layer (Flat Plate at $Re_c = 10e6$ )

- Skin friction



- $u_\tau^2 = -R_{12}|_{eq} = -kb_{12}|_{eq}$
- $c_f$  increases with  $-b_{12}|_{eq}$

- Shear-stress anisotropy



- Target  $b_{12}|_{eq}$  reached for  $0.01 \leq y/\delta_{99} \leq 0.2$

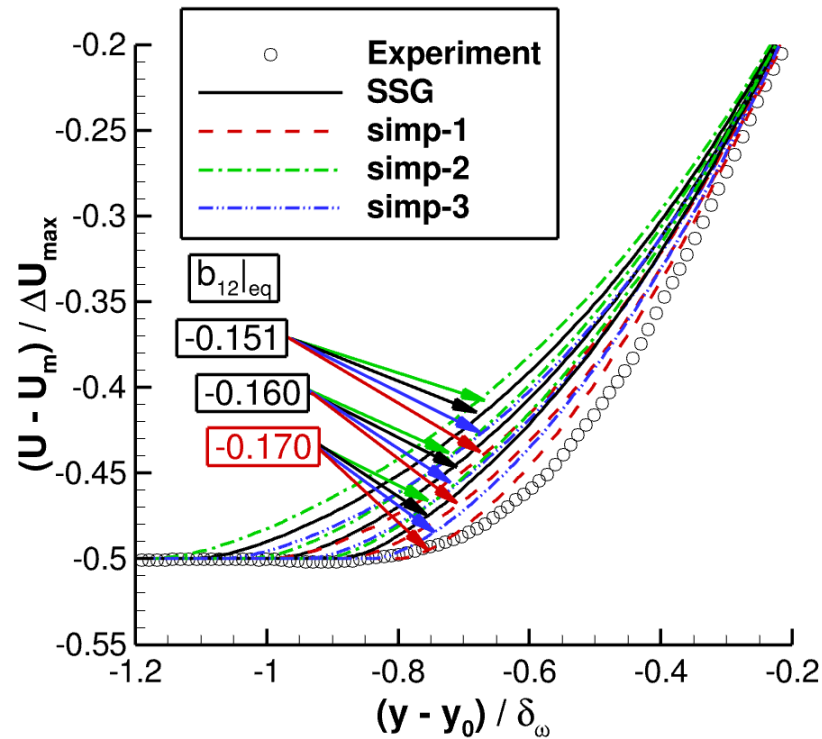
→  $b_{12}|_{eq} = -0.151$  advantageous at high Re



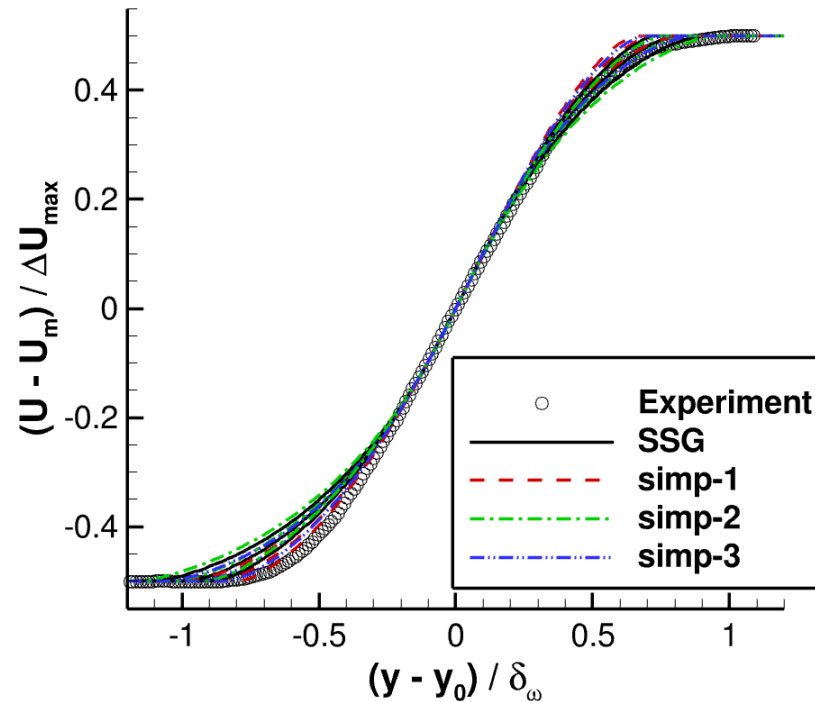
# Simulation Results: Fundamental Flows

## Mixing Layer (Delville et al., 1989) (1)

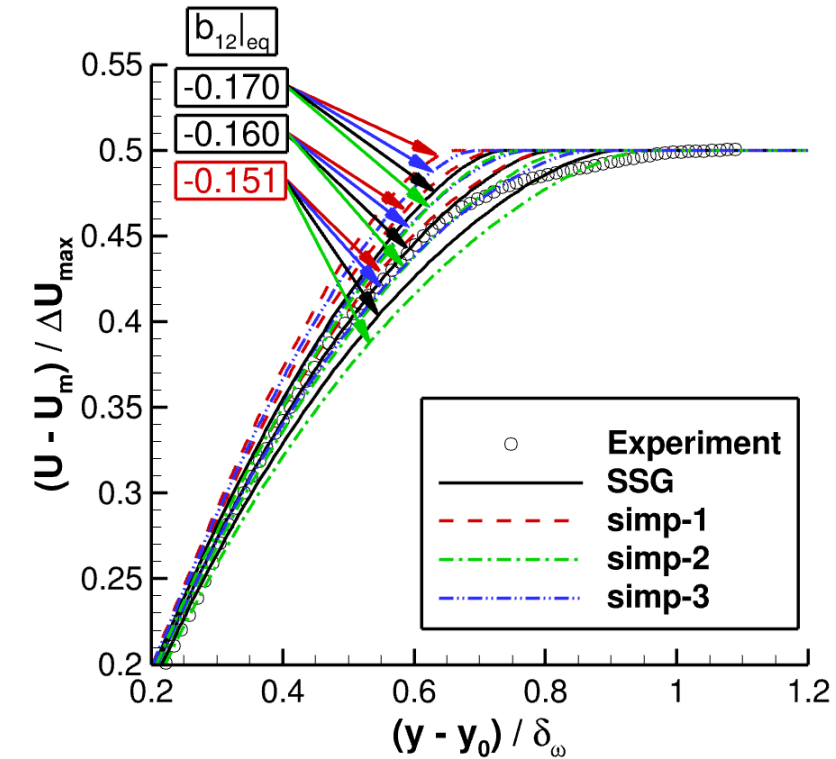
- Velocity profile at  $x = 950\text{mm}$  (most downstream measurement position)



- Lower velocity edge:
- $b_{12}|_{eq} = -0.170$  optimum  
→ high momentum transfer



- Central part (equilibrium state):  
generally good agreement

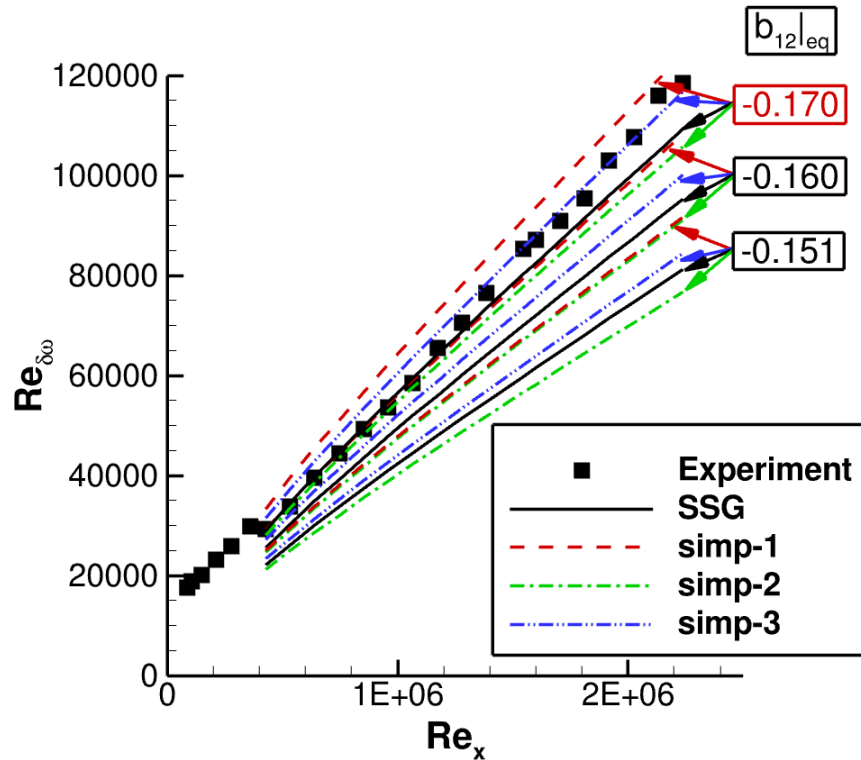


- Higher velocity edge:
- $b_{12}|_{eq} = -0.151$  optimum  
→ low momentum transfer

# Simulation Results: Fundamental Flows

## Mixing Layer (Delville et al., 1989) (2)

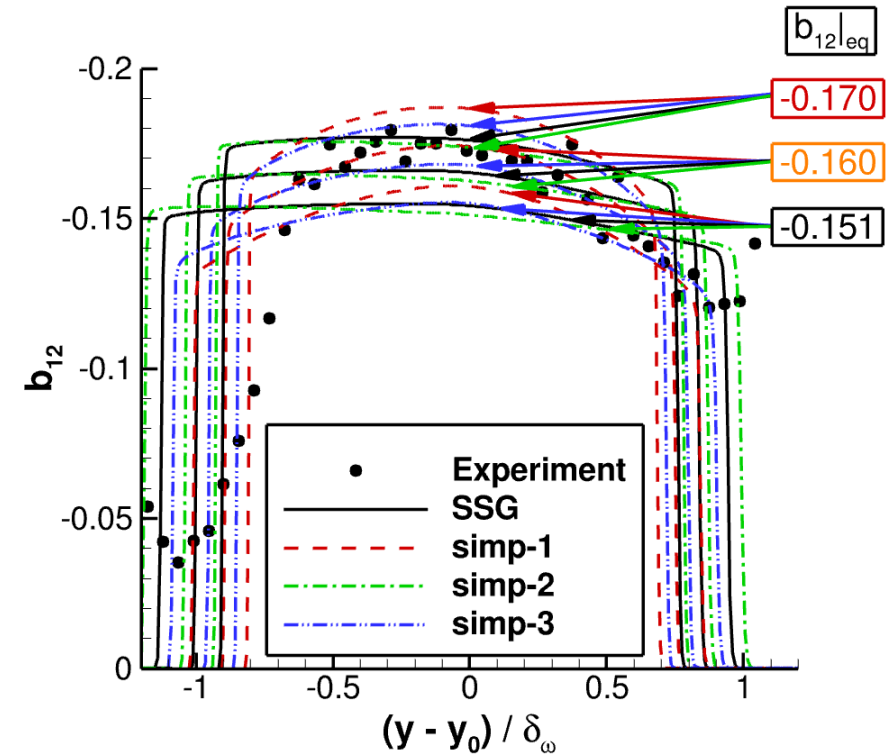
- Spreading



- Equilibrium state defines spreading rate
- Larger variation due to model form
- $b_{12}|_{eq} = -0.170$  optimum

→ Equilibrium state incompatible with boundary layer

- Shear-stress anisotropy at  $x = 950\text{mm}$



- Target  $b_{12}|_{eq}$  reached approximately only  
→ equilibrium state not yet reached  
→ Re too low?



# Overview

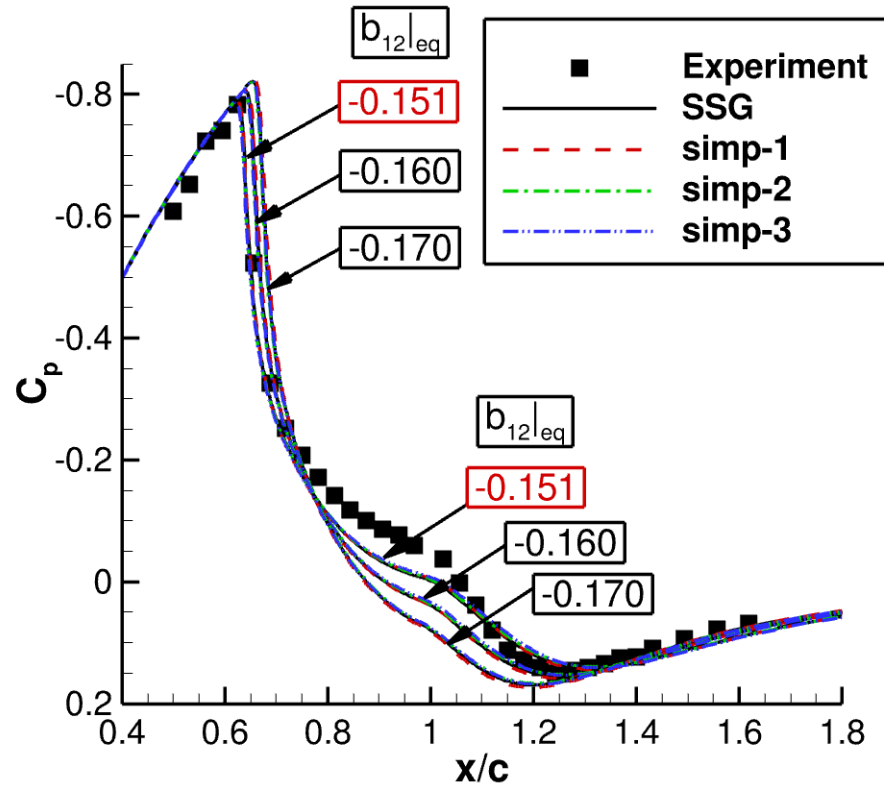
- Introduction
- Theory
- Reynolds Stress Modeling
- **Simulation Results**
  - Fundamental Flows
  - **Applications**
- Potential of Data Driven Methods
- Conclusion



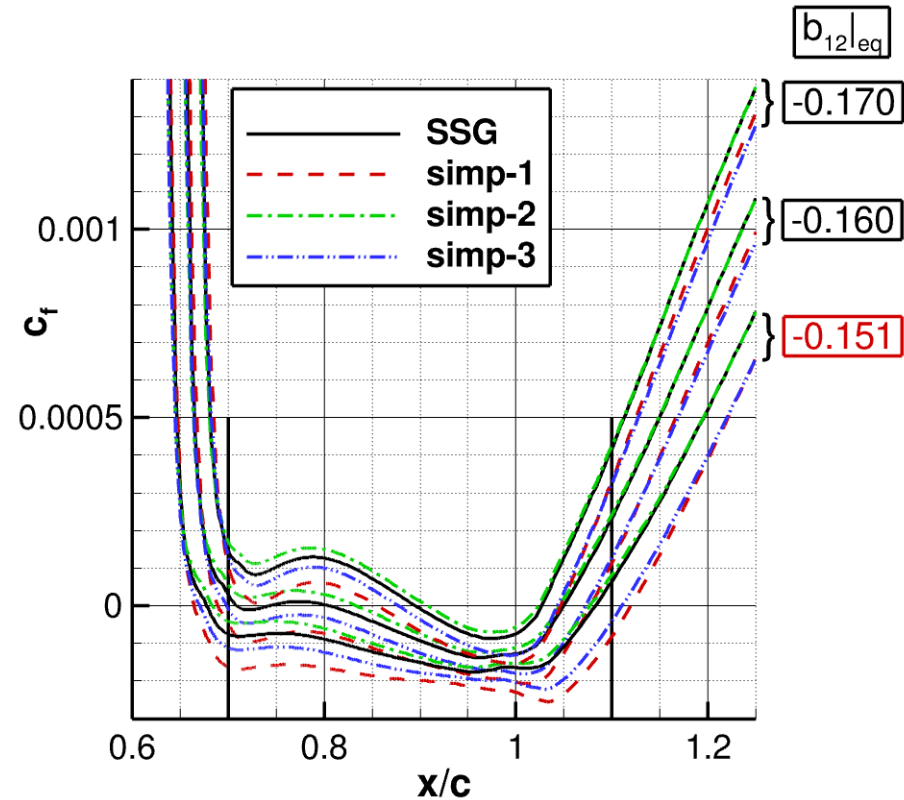
# Simulation Results: Applications

## Axisymmetric Transonic Bump (Bachalo & Johnson, 1986)

- Pressure distribution
- Skin friction in separation region



- Shock position =  $f(b_{12}|_{eq})$
- $b_{12}|_{eq} = -0.151$  optimum (boundary layer)



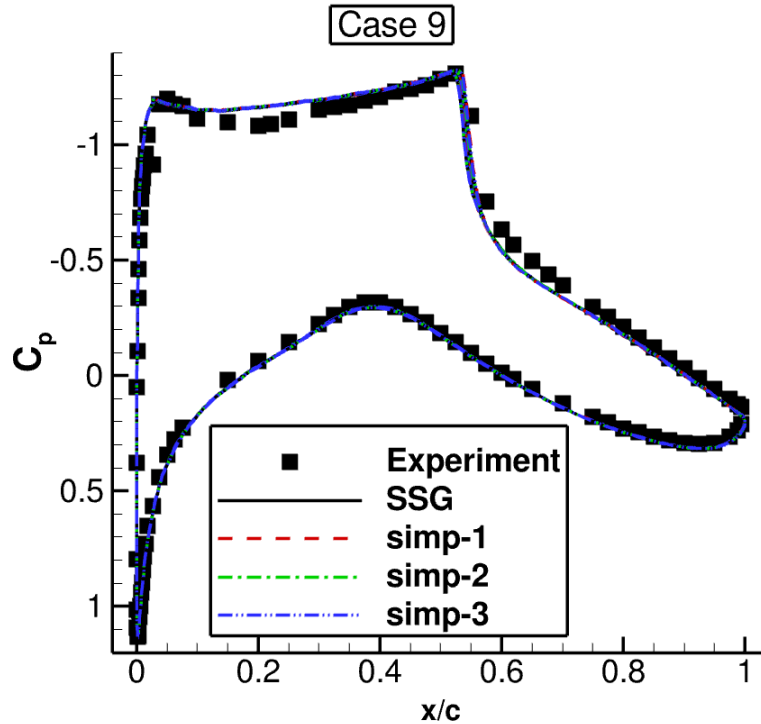
- Minor variation by model form

Results determined by equilibrium state

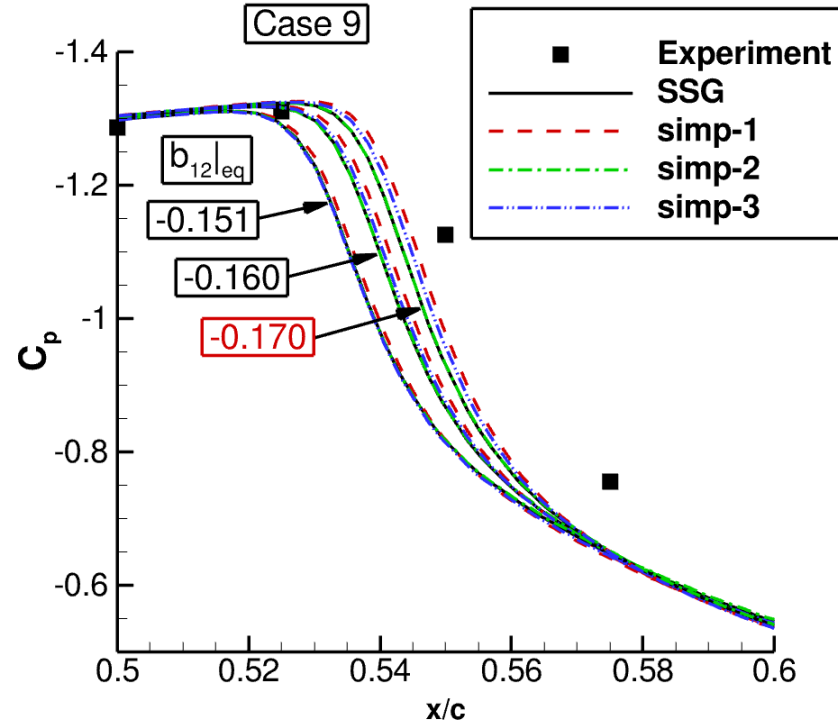
# Simulation Results: Applications

## RAE 2822, Case 9 ( $M = 0.73$ , $Re = 6.5e6$ )

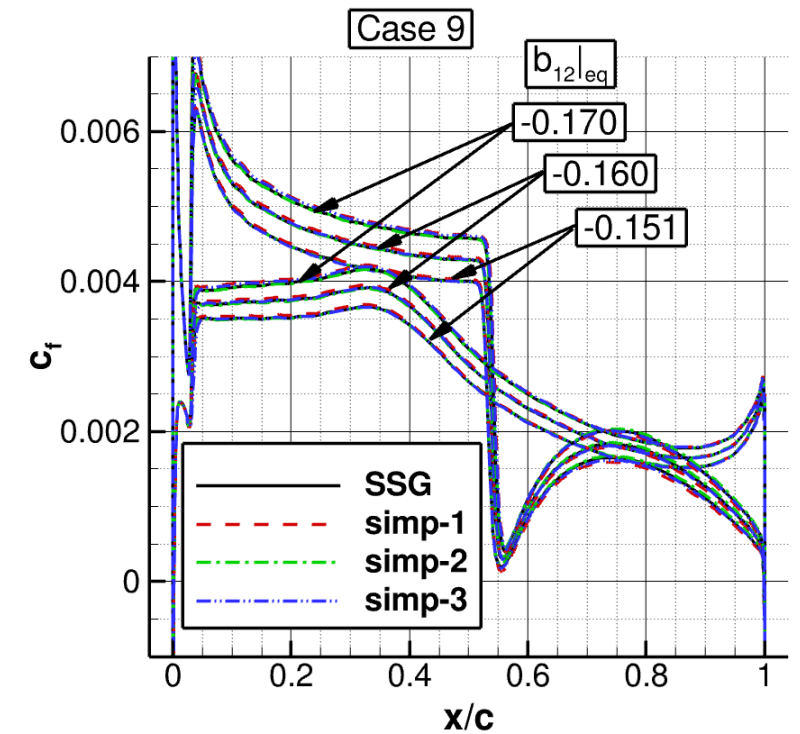
- Pressure distribution
- Pressure distribution, detail
- Skin friction in separation region



- All results similar



- Shock location =  $f(b_{12}|_{eq})$
- $b_{12}|_{eq} = -0.170$  optimum (minor effect)



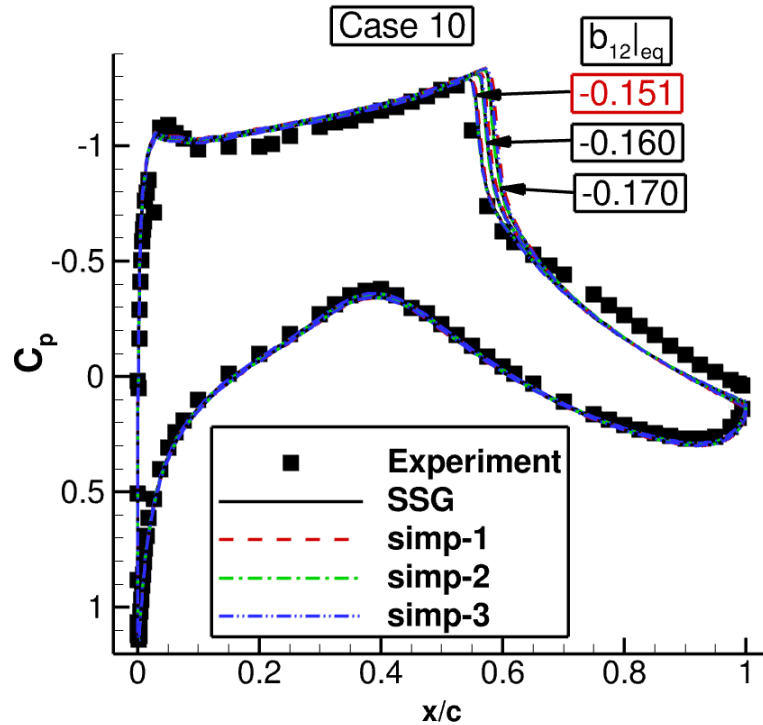
- No separation

Results determined by equilibrium state

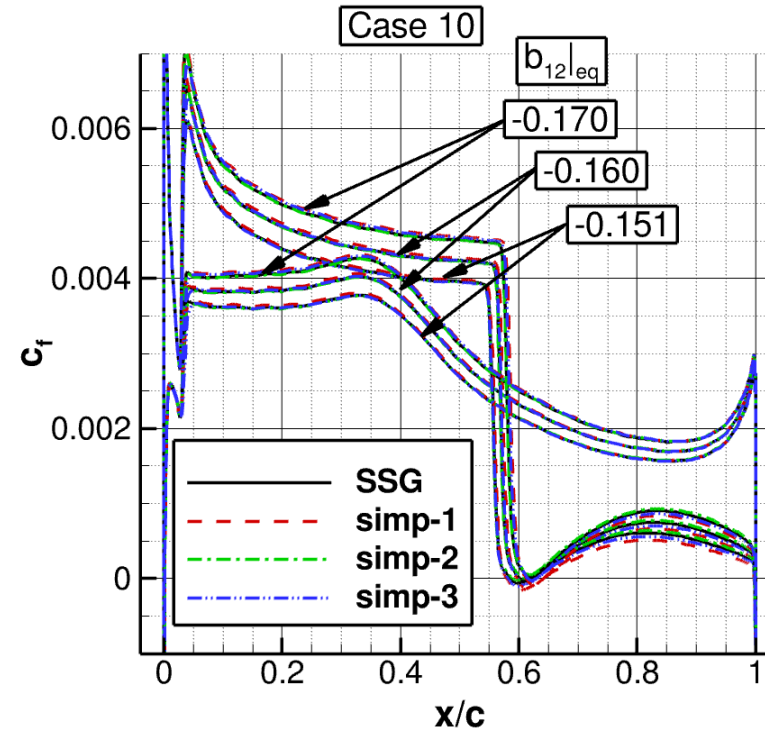
# Simulation Results: Applications

## RAE 2822, Case 10 ( $M = 0.75$ , $Re = 6.2e6$ )

- Pressure distribution
- Skin friction

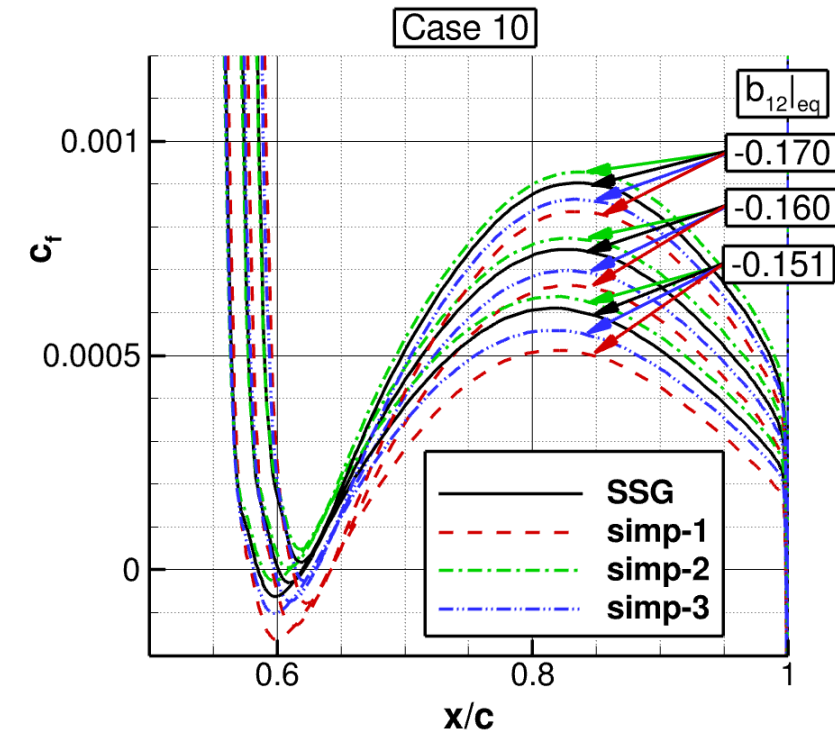


- Shock location =  $f(b_{12|eq})$
- $b_{12|eq} = -0.151$  optimum (major effect)



- Separation =  $f(b_{12|eq})$

- Skin friction in separation region



- $|b_{12|eq}|$  increases  
→ separation reduces

Results determined by equilibrium state

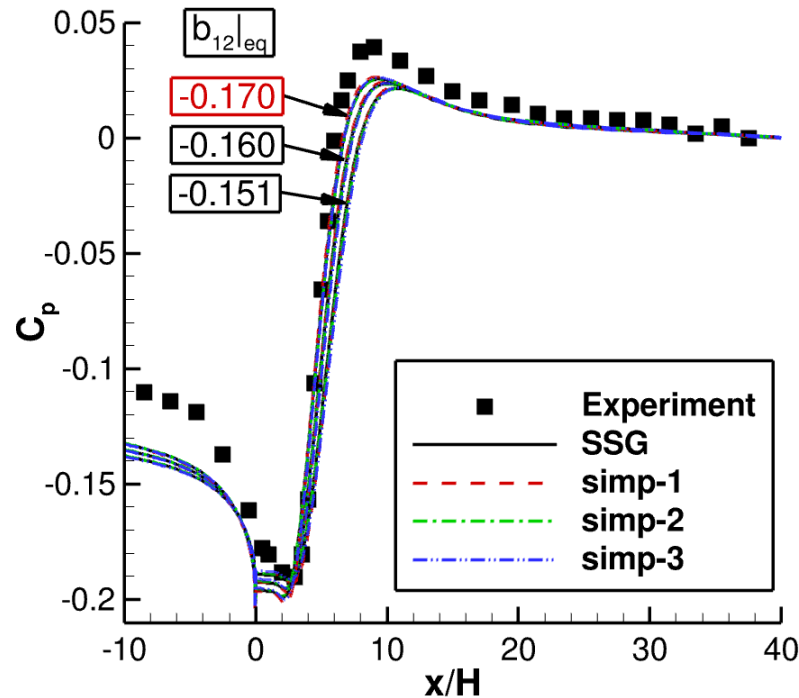
# Simulation Results: Applications

## Backward Facing Step (Driver & Seegmiller, 1985)

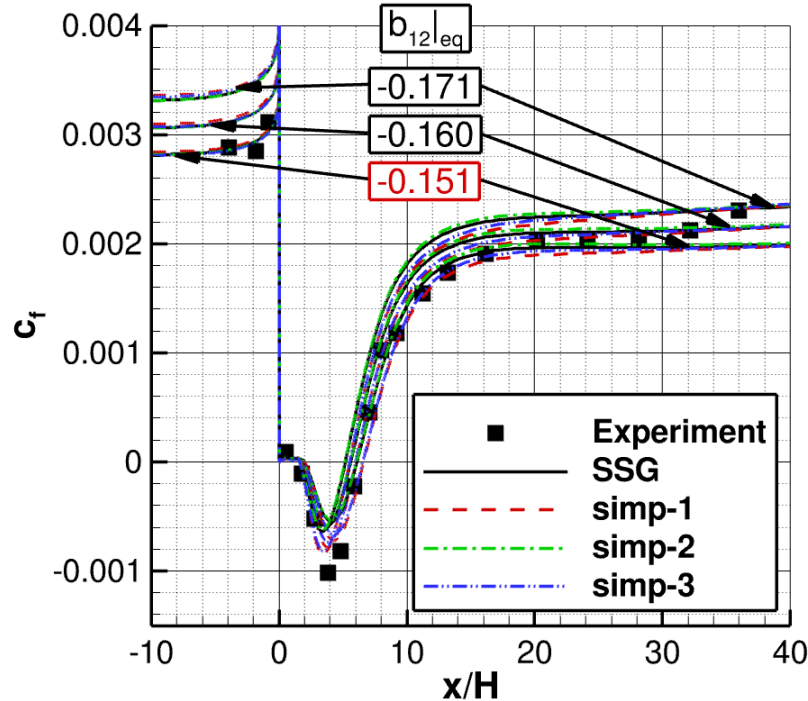
- Pressure distribution

- Skin friction

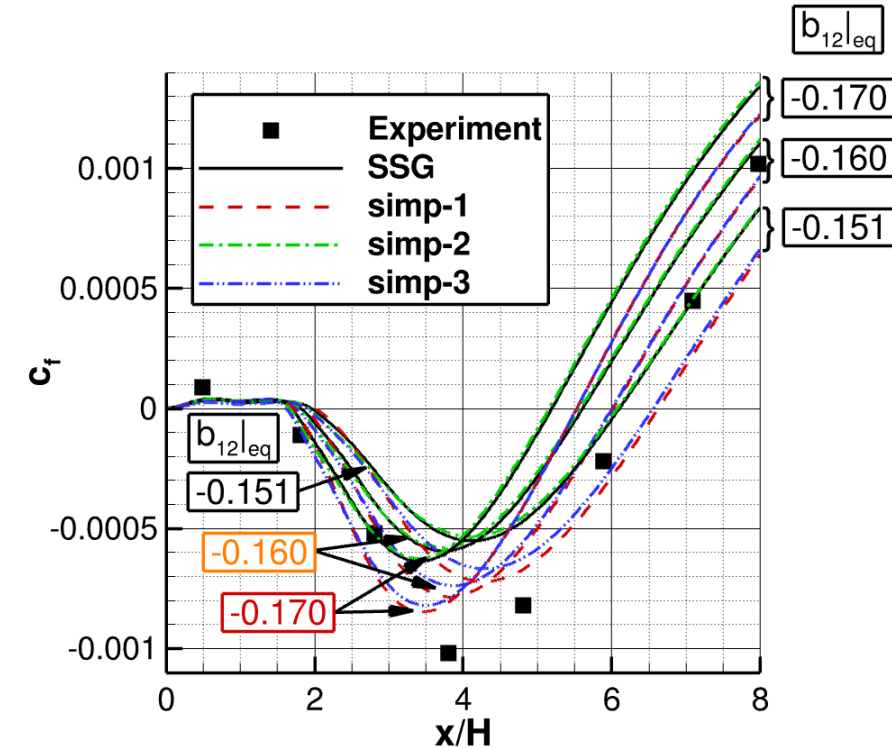
- Skin friction in separation region



- $b_{12}|_{eq} = -0.170$  optimum  
→ mixing layer



- Inflow/recovery:  
 $b_{12}|_{eq} = -0.151$  optimum → BL



- In bubble:  
 $b_{12}|_{eq} = -0.170$  optimum → ML
- Reattachment =  $f(b_{12}|_{eq})$

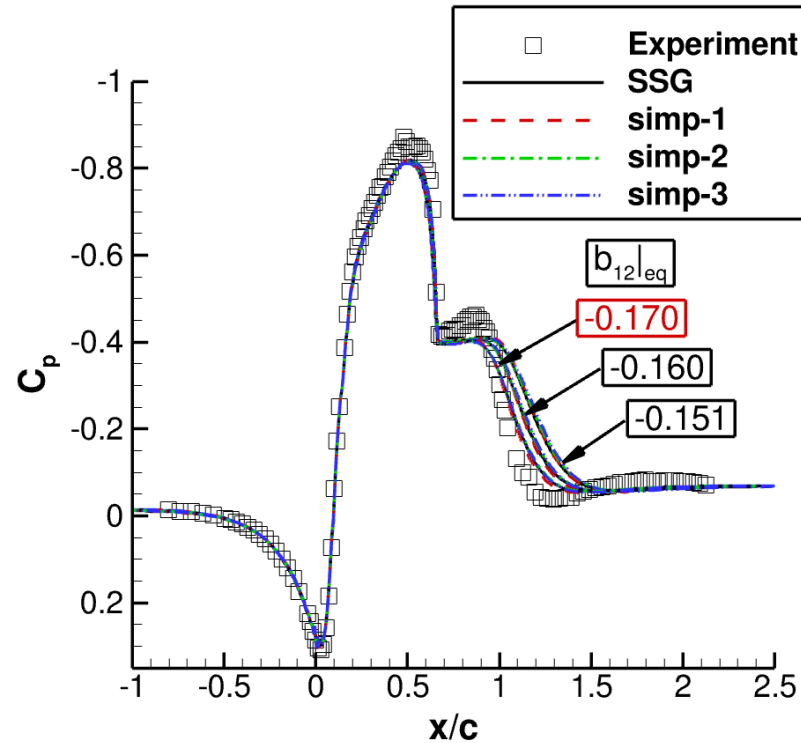
Results determined by equilibrium state



# Simulation Results: Applications

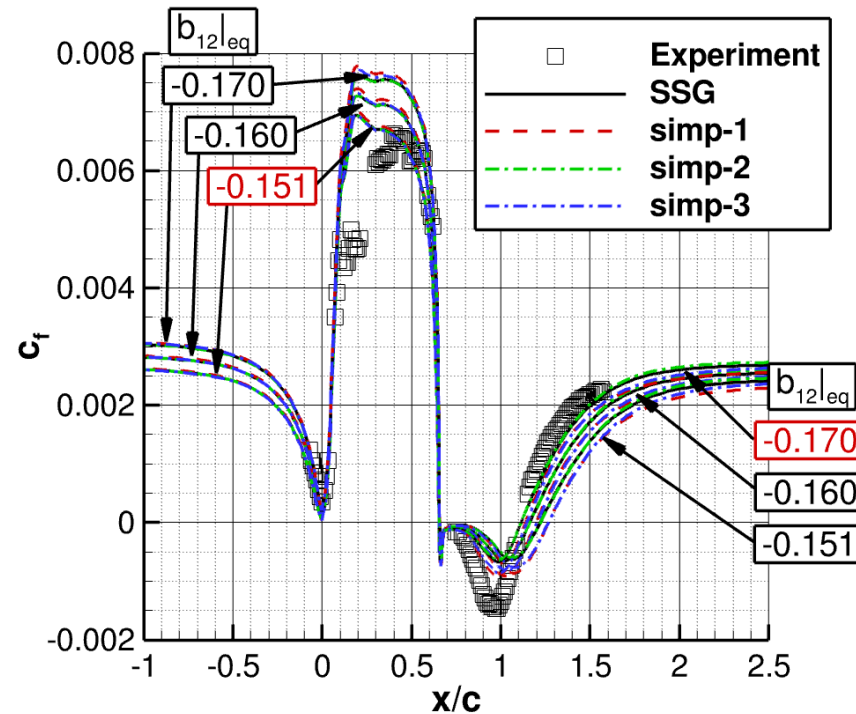
## NASA Hump (Greenblatt et al., 2006)

- Pressure distribution



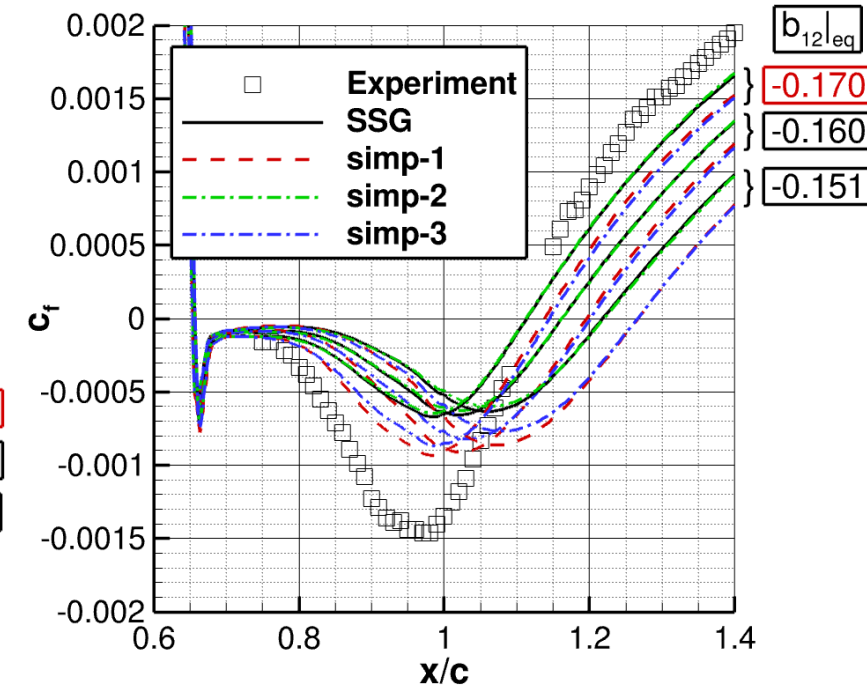
- $b_{12}|_{eq} = -0.170$  optimum  
→ mixing layer

- Skin friction



- Inflow:  $b_{12}|_{eq} = -0.151$  opt. (BL)
- Recovery:  $b_{12}|_{eq} = -0.170$  opt. (ML)

- Skin friction in separation region



- In bubble:  $b_{12}|_{eq} = -0.170$  opt. (ML)
- Reattachment =  $f(b_{12}|_{eq})$

Results determined by equilibrium state

# Overview

- Introduction
- Theory
- Reynolds Stress Modeling
- Simulation Results
  - Fundamental Flows
  - Applications
- **Potential of Data Driven Methods**
- Conclusion

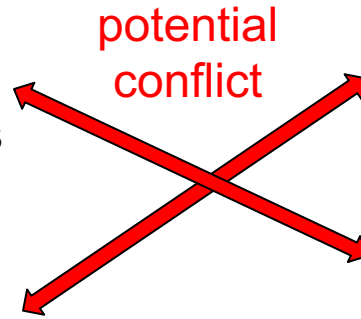




# Potential of Data Driven Methods

## Turbulent Equilibrium

- Modeling
  - Calibration condition
  - Determines model predictions
    - Shock location
    - Separation/reattachment
  - Independent of model form



- Physics
  - Equilibrium state depends on flow
  - Boundary layer  $\neq$  mixing layer

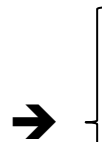
## Data Driven Turbulence Modeling

- Modifications
  - Model coefficients
  - Model terms
- Reference to application data
  - Change of equilibrium state
    - original calibration deteriorated

→ No universal solution

## Potential of DD/ML Technology

- Protect fundamental conditions (Ph. Spalart!!!)
  - classification of local flow type
    - Implicit (selection of parameters/features)
    - Explicit (supervised/unsupervised learning)
- DD/ML outside protected areas



- Maintains previous achievements
- Improvement beyond fundamental flows (unhampered learning)



# Overview

- Introduction
- Theory
- Reynolds Stress Modeling
- Simulation Results
  - Fundamental Flows
  - Applications
- Potential of Data Driven Methods
- Conclusion



# Conclusion

## Reynolds Stress Models

- Turbulent equilibrium → calibration condition for pressure-strain correlation
- Equilibrium state determines model predictions

## Physics

- Equilibrium state depends on flow type

## Potential of Data Driven Methods

- Identification of local flow type (classification) → protection of fundamental conditions
- Modification outside protected areas → improvement beyond fundamental flows



# Conclusion

## Reynolds Stress Models

- Turbulent equilibrium → calibration condition for pressure-strain correlation
- Equilibrium state (and the corresponding Reynolds stress anisotropies) determines model predictions

## Physics

- Equilibrium state depends on flow type (boundary layer vs. mixing layer)
  - Implication for modelling: Different sets of model coefficients for, e.g., boundary layers and mixing layers

## Potential of Data Driven Methods

- Identification of local flow type (classification)
  - Protection of fundamental conditions (e.g., regions of equilibrium state)
  - Inside protected areas:
    - distinguish different equilibrium states with different Rij-anisotropies (boundary layer vs. mixing layer)
    - adaptation of the model coefficients to the local flow type
- Modification outside protected areas → improvement beyond fundamental flows using ML/DD

